RSC Advances

Journal Name

COMMUNICATION

High-yield Synthesis of Graphene Quantum Dots with Strong Green Photoluminescence

J. Gu,[a, b] M. J. Hu,[a] Q. Q. Guo,[a] Z. F. Ding,[c] X. L. Sun[a] and J. Yang[a*]

A facile and high-yield hydrothermal method for synthesizing the graphene quantum dots (GQDs) from glucose was presented. The GQDs, with fluorescence quantum yield (FL QY) of 44.3%, demonstrate strong green photoluminescence (PL) and excitation-independent PL emission characteristics.

Recently, one kind of luminescent carbon nanomaterial-graphene quantum dots (GQDs) has been attracting more and more attention.[1] GQDs are graphene sheets of less than 100nm in size, which have been regarded as a burgeoning functional material due to their unique properties, such as ultraviolet and blue to green luminescence, two-photon induced FL, excellent photo stability, and biocompatibility.[2,3] These superior characteristics distinguish GQDs from the traditional FL materials, and qualify them as promising candidates for the applications in photovoltaics,[4] cell or bio imaging,[5,6] photocatalysis,[7] light-conversion,[3] and sensors.[8]

Two generalized methods, both "top-down" and "bottom-up", have been employed to synthesize GQDs. However, most "top-down" methods are usually unsatisfactory due to the requirements of special equipment, critical synthesis procedures, low QY, or difficulty in controlling the size of products, which seriously affect the PL performance in the application of optoelectronics, photovoltaics, and so on. The "bottom–up" methods, based on carbonizing some special organic precursors via thermal treatment,[9] usually allow accurate control over the morphology, size distribution and lattice dimensions of products. Hence, some suitable molecular precursors either with or without mild surface passivators are chosen to synthesize the luminescent GQDs using one-step hydrothermal pathway.[10-12]

Furthermore, it is of great scientific interest and technological significance to synthesize GQDs with multicolour emissions. The controlled size growth of GQDs has been first used to improve their PL properties, but little success has been achieved primarily due to dominant surface emitting states. Owing to the particular quantum confinement and edge effects, doping of GQDs with chemically bonded atoms could provide more active vacancies and greatly alter their intrinsic characteristics, generating new phenomena and extraordinary performance. Thus, more attention has been then paid to synthesizing multicolour PL GQDs by adding the extraneous elements into the hexagonal matrix of graphene. Some elements such as nitrogen,[13] sulfur,[14] chlorine[15], magnesium,[16] and fluorine[17] have been doped into the hexagonal matrix of grephene during the synthesis process of GQDs. However, few efforts have been made on the development of chlorine-doped GQDs, which may show excellent multicolour PL.

Compared to "top-down" methods, "bottom-up" methods are more cost-effective for production and often result in higher FL QY, which directly determines the FL efficiency. For example, it is reported that Tang *et al.* have ever used glucose as the precursors to synthesize the GQDs through a microwave-assisted hydrothermal method. The GQDs solutions emitted good blue light under 365nm UV and the FL QY of such GQDs was 7~11%, which is slightly higher than the reported values (4~10%) of carbon QDs.[18] But because of its low FL QY and microwave-assisted process, this method is not suitable for industrial-scale production. In order to further improve the FL QY (PL performance) and optimize production process, in our study, a new kind of high-yield green PL chlorine-doped GQDs was synthesized via a facile hydrothermal process using glucose as a low-cost carbon source, which is described in the supporting information (SI, experimental section and Figure S1). Compared with other green PL GQDs reported, the obtained GQDs exhibit much higher FL QY (44.3%) and excitation-independent PL emission.
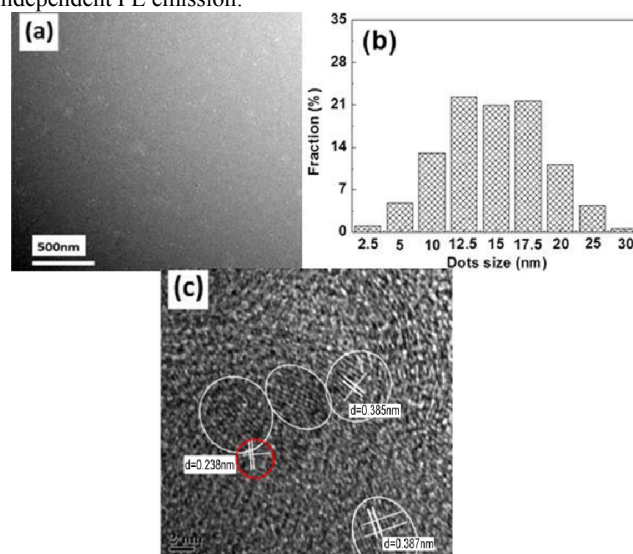
Figure 1 HRTEM images of GQDs. (a) Morphology; (b) Dots size distribution; (c) Lattice fringes

Figure 1a shows the TEM image of obtained GQDs, which can be observed to have a uniform dispersion without apparent aggregation. As shown in Figure 1b, the size distribution of GQDs is in the range of 5~25 nm and the average value is 15 nm. The high crystallinity of GQDs is certified by the HRTEM image (Figure 1c). Well-resolved lattice fringes of 0.386 nm and 0.238 nm for GQDs are the *d* spacing between graphene layers (002 facet) and the in-plane lattice spacing of graphene (100 facet) respectively, which are consistent with the basal plane distance of bulk graphite and the hexagonal lattice.[19] The AFM images of monodisperse GQDs were scanned with atomic force microscope (AFM) (Figure S2a and b) and it is observed that the height of these GQDs mostly distributes in the range from 1.6 to

2.4 nm, with the average height of ~2.0 nm (Figure S2c).

The Raman spectra of obtained GQDs are illustrated in Figure S3. Both a weak G band at 1520 cm^{-1} and a broad D band at 1380 cm^{-1} are observed in Figure S3a. It is generally recognized that the D band results from the vibrations of carbon atoms with dangling bonds in the termination plane of disordered graphite or glassy carbon, while the G band is associated with the E_{2g} mode of the graphite and the vibration of sp^2-bonded carbon atoms in a two-dimensional hexagonal lattice.[20] The intensity ratio (I_D/I_G), which is often applied to correlate the crystal purity and order degree with the graphite, also reveals that the GQDs are mainly composed of graphite. A lower I_D/I_G is found in the Raman spectrum of functionalized graphene sheets (FGS, Figure 1 in Ref. 21) which has lower disorder. Moreover, we think that the D and G bands are also relevant to the atom doping and higher FL QY, so herein the Raman spectrum of another GQDs synthesized by us with higher FL QY (75.2%) is used to assist this analysis (Figure S3b). Typically, only one D band at 1380 cm^{-1} is observed, suggesting that higher FL QY disturbs the Raman analysis of the GQDs. There are more defects, vacancies and edges in the graphene lattice with the introduction of N and Cl atoms, which have changed the lattice fringes, microstructures and FL property of GQDs, leading to the broadening of I_D and apparent disappearance of I_G. However, the Raman spectra and TEM images both verify that obtained GQDs have the crystalline structure features of graphene.

The surface groups and chemical compositions of obtained GQDs were further analysed by XPS and FTIR spectra. Figure S4a shows the full scan XPS spectrum of GQDs. Three obvious 1s orbital peaks are detected at ~284 eV (C1s), ~400 eV (N1s) and ~530 eV (O1s) respectively, indicating these three elements (C, N, O) are enriched on the surface of GQDs. The N1s XPS signal arises from the ethylenediamine (EDA), and the O1s XPS signal is relatively high due to the contribution from the substrate SiO$_2$. Meanwhile, a 2p orbital peak at ~201 eV (Cl2p) is also detected, suggesting there is also Cl element on the surface of GQDs. As seen in Figure S4b, the C1s XPS spectrum can be deconvoluted into four small peaks centred at 284.5 eV, 286.6 eV, 288.2 eV and 289.4 eV respectively, corresponding to four different types of carbon bonds (graphitic and aliphatic (C–C/C=C), oxygenated, nitrous and chlorine carbon). The relative contents of these elements are listed in Table S1, from which we can see that C–C/C=C are the dominant functional groups (C1s=57.2 at.%), and the C–Cl bond in the C1s XPS spectrum is directly related to the Cl doping. The Cl2p XPS spectrum (Figure S4c) is split into two peaks centred at 200.8 eV and 202.2 eV, which are respectively the binding energies of Cl2p$_{3/2}$ and Cl2p$_{1/2}$ due to the spin-orbit splitting of Cl2p core level (1.6 eV).[22]

In the FTIR spectrum of GQDs (Figure S4d), the following peaks are observed: the stretching vibration peaks of C–OH at 3421 cm^{-1} and C–H at 2929 cm^{-1}, as well as a vibrational absorption peak of C=O conjugated with condensed aromatic carbons at 1627 cm^{-1}. These data reveal that the obtained GQDs are rich in carboxylic groups, while the weaker absorption peak of C=O indicates a decrease of O content after the reactants are dehydrated. The symmetric stretching vibration peak of C–NH–C lies in 1220 cm^{-1},[23] which indicates there are interactions between N and H, suggesting the presence of N element on the surface of GQDs (as shown in Figure S4a). In addition, it is evident that there are two absorption peaks at around 801 cm^{-1} and 1713 cm^{-1}. The band at 801 cm^{-1} ascribes to the vibration of C–Cl. The band at 1713 cm^{-1} can be assigned to the formation of C=C–Cl/C=C–O, which demonstrates the effectiveness of Cl atom doped into GQDs atomic lattice (C–Cl) and the formation of an unsaturated graphene C=C structure during the carbonization process.

The UV-Vis spectrum and FL spectra of obtained GQDs aqueous solution are illustrated in Figure 2. In Figure 2a, there is one obvious absorption peak at 250 nm, which derives from π-π* transition of the aromatic sp^2 domains. The broadened peak at around 300 nm may be attributed to n-π* transition of C=O bond [24] and the trapping of excited-state energy by the surface states resulting in strong emission. A broad emission peak at 524 nm, which is within the emission wavelength range of the green light, is observed when the GQDs solution is excited at 250 nm. In the FL spectra of GQDs (Figure 2b), the FL emission peak positions have almost no shift with the increase of UV excitation wavelength from 320 nm to 440 nm. This excitation-independent PL characteristic of obtained GQDs is different from that of most FL carbon-based materials, implying that the PL of obtained GQDs is more dependent on the surface states than the size, and the emission sites of the sp^2 clusters should be fairly uniform. As shown in the inset of Figure 2b, the GQDs solution emits strong green PL under a hand-held 365 nm UV light in contrast to the transparent colour under visible light. Therefore, it is believed that the green PL is produced by the ordered sp^2 clusters as the GQDs contain abundant sp^2 structures, [25] oxygenated, nitrous carbon groups. It is further noteworthy that the green PL also partially results from the incorporation of 2p orbital Cl atoms into the graphene lattice, which changes the surface states of GQDs (providing more "defect sites"). These "defect sites" directly make the trapping of excitation energy more efficiently and result in strong green emission.
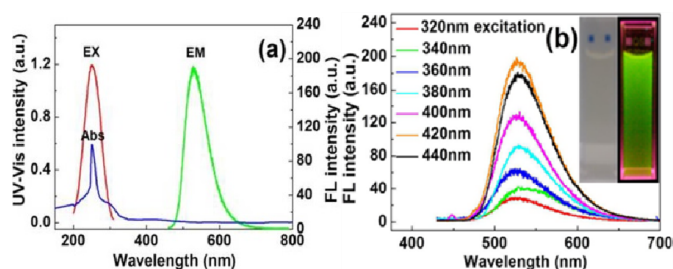
Figure 2 (a) UV-Vis spectrum (blue line) and FL spectra (red and green lines) of obtained GQDs; (b) Typical FL spectra of obtained GQDs, and photos of the GQDs solution under visible (left) and 365 nm UV (right) light

According to Equation (1) in the SI, the UV-Vis intensity, FL intensity of the GQDs aqueous solution and QS/0.1M H$_2$SO$_4$ solution with different concentrations were measured (Table S2) to calculate the FL QY of obtained GQDs. The FL intensity with respect to UV-Vis intensity is illustrated as Figure S5. The FL QY of obtained GQDs is determined to be 44.3% (Table S3), as calculated by the slopes of two fitting lines, which is much higher than that of the conventional green PL GQDs (≤15%) reported.[5]
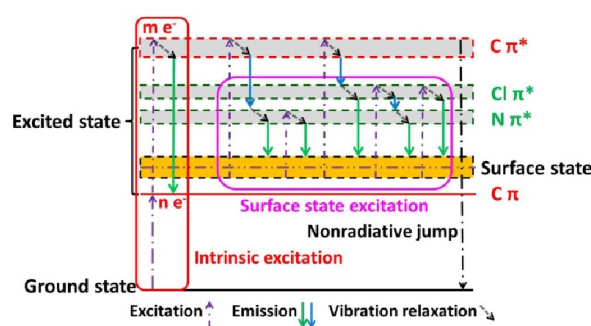
Figure 3 Diagram of energy levels and the electronic transitions in the GQDs

It is affirmative that the dehydration and carbonization processes promote the formation of cyclic aromatic hydrocarbon-like conjugated structure. Firstly, the green PL is due to the synergistic effect of C=C core emission (the π–π* electron transition of C=C) [25] and the surface/molecule states, which remarkably influence the band gap (energy levels) and surface states of GQDs, leading to the improvement of green PL performance. The energy of the functional groups on the surface forms the "surface states" which are the energy levels between C π and C π*. Because of the difference in chemical bonding between C=C and C=O groups, the vibration of π* energy states is expected, and a distribution of π* band (C=C and C=O) is also acquired. Schematic diagram of the energy levels and electronic transitions in the GQDs is depicted in Figure 3. Then, the presence of N1s introduces a new N π* level (obvious N–C=O group as shown in Figure S4b) between the surface state and C π*, which causes the blue PL emission from C π* to N π* when the GQDs are illuminated with certain energy.[25] The excitons are subsequently released to surface state by vibration relaxation and generate the green PL emission. In addition, the excitons can also be excited to N π* directly and then generate the green PL emission when they are released to surface state. Hence, the presence of N is considered to play another important role for the green PL of GQDs because the FL QYs are generally less than 15% if there are only oxygenated groups (–OH and –COOH). Just as one or more N-containing groups (N–C=O, even a few –NH$_2$) are present, the FL QYs of most GQDs can be over 15% (FL QY can be up to 70%~80% under optimal synthesis process).[2] Notably, the incorporation of 2p orbital Cl atoms into GQDs also greatly increases the green PL by increment of more "defect sites" as well as an additional energy level Cl π* between N π* and C π*, which effectively creates new electron transition pathways in the band structure of GQDs (as shown in Figure 3). Owing to the existence of Cl π* level, the excitons can be released in two ways. One is through direct recombination after vibration relaxation (Cl π*→surface state), generating green PL. The other is undergoing intersystem crossing (C π*→Cl π* and Cl π*→surface state, Cl π*→N π* and N π*→surface state), followed by vibration relaxation and ultimately radiative recombination occurs. These two ways lead to the increase of green PL from surface states emission and the enhancement of the tunability of emission wavelength. In addition, carbon atoms occupied by the doping atoms also reduce the agminated aromatic-rich carbon-domains, leading to the increase of the FL QY. All of these factors jointly make the FL QY of GQDs be much higher than that of the conventional green PL GQDs, which will inevitably improve the optical characteristics of optoelectronics, LED emission, bioimaging and sensors in the near future.

In order to investigate the sensitivity of GQDs to visible light, the effect of the exposure time under visible light on the green PL and FL QY of obtained GQDs was further analysed, as shown in Figure S6. The FL QY of GQDs has almost no change (43.8%~45.0%) with the exposure time from 0 to 75 days. Inset of Figure S6 exhibits the photos of the GQDs aqueous solution under the 365 nm UV light with corresponding exposure time, and it is difficult to observe the variation of green PL. Therefore, it is believed that the effect of the exposure time under visible light on the green PL and FL QY of GQDs is quite insignificant, which means obtained GQDs are highly stable under natural environmental conditions.

Because most of luminescent materials are only water-soluble, the solubility and PL performance of obtained GQDs in different solvents were investigated. The photos in Figure S7 demonstrate that obtained GQDs can also be dissolved well in these five organic solvents besides the DI-water, which is better than the solubility of the GQDs reported. We deduce that the doping atoms may improve the affinity of the GQDs with these organic solvents. It is further found that there is green PL in the GQDs/DI-water, GQDs/PVA and GQDs/ethanol solutions under the 365 nm UV light, while no PL performance is observed in the other solutions containing acetone, DMF and glycerol. The PL mechanism of GQDs in different solvents still remains unclear. As most GQDs do have the PL performance only in the aqueous solution, the PL performance of obtained GQDs in different solvents will make it very useful in non-aqueous conditions.

In summary, a facile and high-yield hydrothermal method for the synthesis of GQDs using low-cost source materials was developed. This method is suitable for industrial-scale production. The obtained GQDs are about 15 nm in size with distinct lattice fringes of grapheme, and these GQDs exhibit strong green PL under the 365 nm UV light. It is extremely important that the GQDs have high FL QY and excitation-independent PL emission characteristics. Especially, the FL QY of GQDs is up to 44.3%, which is much higher than that of the conventional green PL GQDs. It is understood that the band gap and surface states both play the leading role in the PL of GQDs with cyclic aromatic hydrocarbon-like conjugated structure. In this method, the doping of N and Cl atoms greatly increases the FL intensity by introduction of more "defect sites" and additional energy levels, effectively creating new electron transition pathways in the band structure of GQDs. Meanwhile, carbon atoms occupied by the doping atoms reduce the agminated aromatic-rich carbon-domains, leading to a dramatic increase of the FL QY. Thus, it is reasonable to believe that these high-yield GQDs with strong green PL will bring more opportunities for their applications in the fields of optoelectronics, LED emission, bioimaging and beyond.

Notes and references

1 Y. Q. Dong, J. W. Shao, C. Q. Chen, H. R. Li, X. Wang, Y. W. Chi, X. M. Lin and G. N. Chen, *Carbon*, 2012, **50**, 4738.

2 S. J. Zhu, Q. N. Meng, L. Wang, J. H.Zhang, Y. B. Song, H. Jin, K. Zhang, H. C. Sun, H. Y. Wang and B. Yang, *Angew. Chem. Int. Ed.*, 2013, **52**, 3953.

3 Y. Li, Y. Hu, Y. Zhao, G. Q. Shi, L. R. Deng, Y. B. Hou and L. T. Qu, *Adv. Mater.*, 2011, **23**, 776.

4 V. Gupta, N. Chaudhary, R. Srivastava, G. D. Sharma, R. Bhadwaj and S. Chand, *J. Am. Chem. Soc.*, 2011, **133**, 9960.

5 X. T. Zheng, A. Than, A. Ananthanaraya, D. H. Kim and P. Chen, *ACS Nano*, 2013, 7, 6278.

6 S. J. Zhu, J. H. Zhang, C. Y. Qiao, S. J. Tang, Y. F. Li, W. J. Yuan, B. Li, L. Tian , F. Liu and R. Hu, *Chem. Commun.*, 2011, **47**, 6858.

7 S. J. Zhuo, M. W. Shao, and S. T. Lee, *ACS Nano*, 2012, **6**, 1059.

8 J. Zhao, G. F. Chen, L. Zhu and G. X. Li, *Electrochem. Commun.*, 2011, **13**, 31.

9 X. Yan, X. Cui, B. S. Li and L. S. Li, *Nano Lett.*, 2010, **10**, 1869.

10 Y. H. Yang, J. H. Cui, M. T. Zheng, C. F. Hu, S. Z. Tan, Y. Xiao, Q. Yang and Y. L. Liu, *Chem. Commun.*, 2012, **48**, 380.

11 X. Y. Zhai, P. Zhang, C. J. Liu, T. Bai, W. C. Li, L. M. Dai and W. G. Liu, *Chem. Commun.*, 2012, **48**, 7955.

12 L. W. Sun, J. Zhao, L.J. Zhou and G. D. Li, *Chem. Commun.*, 2013, **49**, 6087.

13 Q. Q. Li, S. Zhang, L. M. Dai and L. S. Li, *J. Am. Chem. Soc.*, 2012, **134**, 18932.

RSC Advances Accepted Manuscript

14 J. Liang, Y. Jiao, M. Jaroniec and S. Z. Qiao, *Angew. Chem. Int. Ed.*, 2012, **51,** 11496.

15 X. M. Li, S. P. Lau, L. B. Tang, R. B. Ji and P. Z. Yang, *J. Mater. Chem. C*, 2013, **1**, 7308.

16 F. Li, C. J. Liu, J. Yang, Z. Wang, W. G. Liu and F. Tian, *RSC Adv.*, 2014, **4,** 3201.

17 X. J. Sun, Y. W. Zhang, P. Song, J. Pan, L. Zhuang, W. L. Xu and W. Xing, *ACS Catal.*, 2013, **3,** 1726.

18 L. B. Tang, R. B. Ji, X. K. Cao, J. Y. Lin, H. X. Jiang, X. M. Li, K. S. Teng, C. M. Luk, S. J. Zeng, J. H. Hao and S. P. Lau, *ACS Nano*, 2012, **6**, 5102.

19 L. Biedermann, M. Bolen, M. Capano, D. Zemlyanov and R. Reifenberger, *Phys. Rev. B*, 2009, **79,** 125411.

20 S. Lijima, *Nature*, 1991, **354,** 56.

21 K. N. Kudin, B. Ozbas, H. C. Schniepp, R. K. Prud'homme, I. A. Aksay and R.Car, *Nano Lett.*, 2008, **8,** 36.

22 R. Graupner, J. Abraham, A. Vencelova, T. Seyller, F. Hennrich, M. M. Kappes, A. Hirsch and L. Ley, *Phys. Chem. Chem. Phys*., 2003, **5,** 5472.

23 D. Y. Pan, J. C. Zhang, Z. Li, C. Wu, X. M. Yan and M. H. Wu, *Chem. Commun.*, 2010, **46,** 3681.

24 G. Eda, Y. Y. Lin, C. Mattevi, H. Yamaguchi, H. A. Chen, I. S. Chen, C. W. Chen and M. Chhowalla, *Adv. Mater.*, 2010, **22**, 505.

25 M. A. Sk, A. Ananthanarayanan, L. Huang, K. H. Lim and P. Chen, *J. Mater. Chem. C*, 2014, **2**, 6954.

Corresponding author: *Jun Yang, Department of Mechanical & Materials Engineering, The University of Western Ontario, London, ON, Canada, N6A 5B9; Tel.: +1-519-661-2111 ext. 80158; fax: +1-519-661-3020. E-mail address: jyang@eng.uwo.ca (J. Yang).*